Semiconductors, 2025, Vol. 59, No. 9

Photoinduced band-gap renormalization in degenerate narrow-gap *n*-InGaN epitaxial films

© K.E. Kudryavtsev, B.A. Andreev, D.N. Lobanov, M.A. Kalinnikov, A.V. Novikov, Z.F. Krasilnik

Institute of Physics of Microstructures, Russian Academy of Sciences,
603087 Nizhny Novgorod, Russia

E-mail: konstantin@ipmras.ru

Received November 19, 2025
Revised November 29, 2025
Accepted December 1, 2025

Based on the analysis of low-temperature stimulated emission spectra, conclusions are drawn about the band gap narrowing effect (ΔE_{BGN}) in degenerate, $n \sim 10^{19}\,\mathrm{cm}^{-3}$, epitaxial InGaN films with an indium content of 60 % under intense photoexcitation. A red shift of the generation line is demonstrated due to the large ΔE_{BGN} exceeding $2\,\mathrm{meV}/10^{17}\mathrm{cm}^{-3}$, apparently provided by the Coulomb interaction of degenerate (equilibrium) electrons and nonequilibrium holes localized in the local extrema of the fluctuating band potential, with limited contribution from exchange (Hartree-Fock) interaction. This behavior directly determines the features of the competition between modal gain and losses in bulk In(Ga)N films. The obtained results can also be projected onto promising low-dimensional structures for red-range quantum wells emitters with based on „intermediate composition" InGaN.

Keywords: indium gallium nitride, stimulated emission, band-gap renormalization.

DOI: 10.61011/SC.2025.09.62835.8795

1. Introduction

Despite significant progress both in the technology of epitaxial growth of III-nitrides [1–3] and in the diagnosis of the resulting structures, the InGaN material system remains quite complex. Thus, not too thick ($\sim 1\,\mu$m or less) bulk films of binary InN and indo-enriched ternary InGaN solutions are still characterized by very high defects and strong, ranging up to $10^{18}-10^{19}\,\mathrm{cm}^{-3}$, background doping of the *n*-type. Combined with the low effective mass of electrons, this leads to a significant manifestation of the Burstein-Moss effects and band gap renormalization, which determine multidirectional energy shifts (hereinafter ΔE_{F} and ΔE_{BGN}, respectively) in the photoreceptor spectra. In the framework of the simplest approximations, the dependence of the Burstein-Moss shift on the electron concentration n has the form $\Delta E_{\mathrm{F}} \sim n^{2/3}$ [4]. Several components contribute to the renormalization of the zone, which is well described, for example, in Ref. [5]. These are the exchange interaction of the main charge carriers ΔE_{exch}, the correlation contribution of the electron-hole interaction ΔE_{corr}, and the interaction of carriers with impurity centers ΔE_{e-i}. The concentration dependences of these terms have the form $\sim n^{1/3}$, $\sim n^{1/4}$ and $\sim n^{1/2}$, respectively [5,6], and since all these dependences are weaker than $n^{2/3}$ in magnitude ΔE_{F}, in the limit of large n, the emission band and the edge of the interband absorption shift to the blue side: $\Delta E_{\mathrm{F}} > |\Delta E_{\mathrm{BGN}}|$.

For relatively new III-N materials, the effects of band renormalization have been studied to a much lesser extent in comparison with „classical" semiconductors such as, for example, GaAs, GaSb, InSb or InP. While the quantitative estimates for GaN ΔE_{BGN} presented in various papers [7–9] are generally similar, the data for InN, on the contrary, are extremely heterogeneous [10–12]. It should also be noted that in the overwhelming number of works considering spectral shifts of the InN luminescent response, the main attention was paid to the role of the equilibrium concentration of electrons. The dynamic component of the effect associated with intensive pumping was noted primarily in experiments using the „pumping-sensing" technique (for example, [13–15]) only at a qualitative level. As for InGaN ternary solutions, the issue of zone renormalization has been raised in a significant number of papers on heterostructures with InGaN/GaN quantum wells [16,17], however, only for sufficiently wide-band structures in the blue range and shorter wavelengths. No such studies have been conducted for InGaN with a high ($> 30-40$ %) proportion of indium.

In this paper, the competition of the effects of electronic state flooding and band gap narrowing in InGaN epitaxial layers with a fraction of indium $x_{\mathrm{In}} \sim 60$ % in the mode of intense optical pumping is experimentally studied. The choice in favor of relatively „wide-band" InGaN rather than InN structures is due, among other things, to current trends: InGaN red-band LEDs are currently one of the hottest trends in the III-nitride field [18–20], and their effectiveness in developing high-resolution full-color displays exceeds that of AlGaInP. The excitation power is selected large enough so that the achievable nonequilibrium concentrations ($\delta n \sim 10^{18}\,\mathrm{cm}^{-3}$) correspond to typical operating concentrations in InGaN LEDs [21]. At low temperatures, such values of δn are higher than the thresholds for the occurrence of stimulated radiation (SR) in the studied InGaN layers, and in this paper conclusions about the magnitude of the band gap renormalization are made based on the analysis of the spectra of stimulated emission, while consideration of spontaneous emission (photoluminescence,

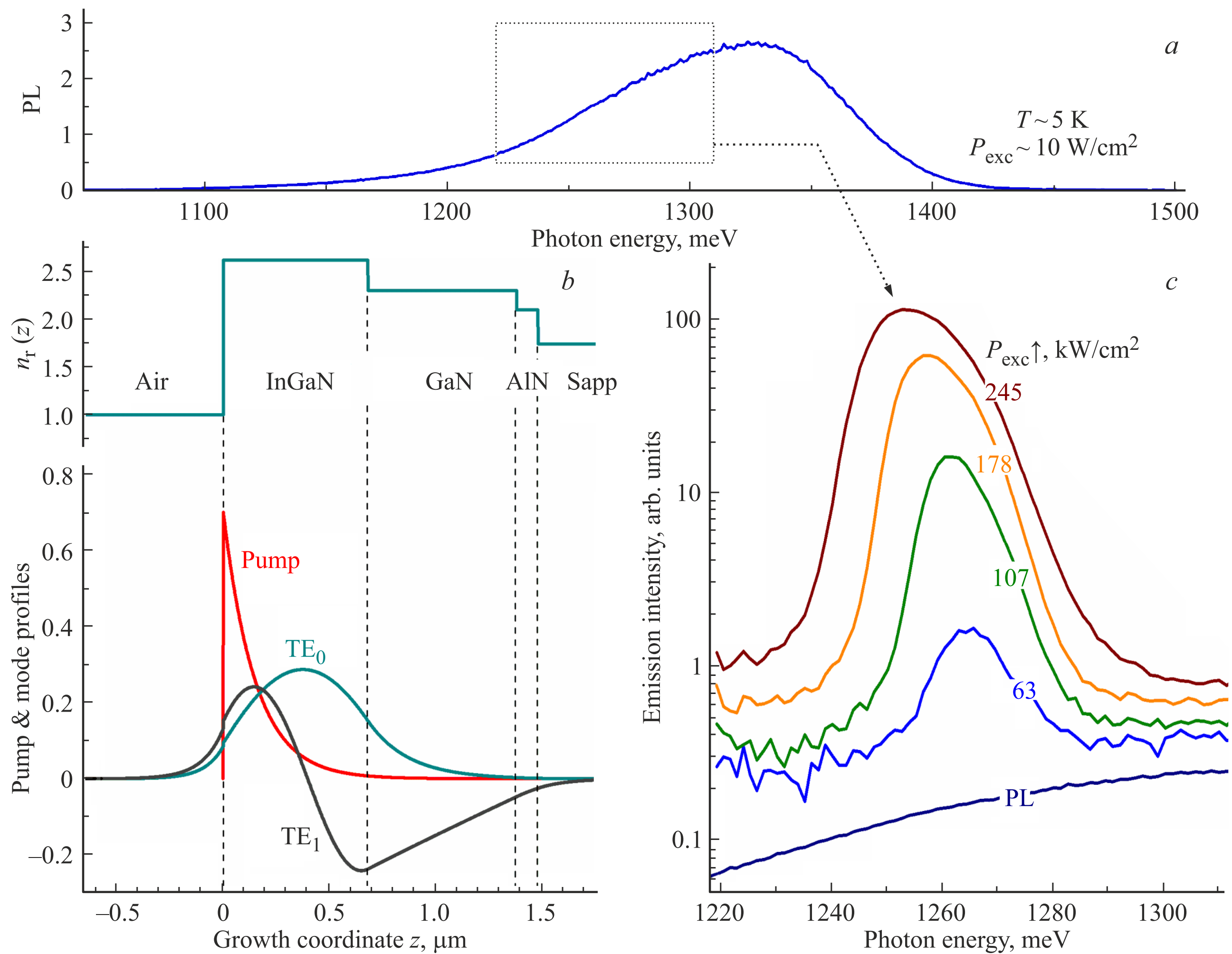

Figure 1. *a* — the PL spectrum of a sample with an active layer $In_{0.6}Ga_{0.4}N$, measured at low temperature in the weak pumping mode when registering PL from the front surface of the structure. The spectral bandwidth of luminescence (at half-height) exceeds 100 meV. *b* — above: growth diagram of the sample under study — deposited layers and refractive index profile; below: profiles of radiation absorption (pump) and field distribution of waveguide modes most likely involved in stimulated radiation processes — the main TE_0-mode and the excited TE_1. *c* — SI spectra as a function of the pumping power density recorded during observation from the end of the structure. For comparison, the spectrum of spontaneous emission (PL) is shown (off-scale).

PL) may be less accurate due to the large (> 100 meV, Figure 1, *a*) spectral width of the photo response.

2. Experimental procedure

The studied structures obtained on c-Al_2O_3 substrates by molecular beam epitaxy with plasma nitrogen activation consisted of buffer layers AlN,(100 nm)/GaN (700 nm) and an active layer of $In_{0.6}Ga_{0.4}N$ (680 nm); the corresponding growth scheme is shown in Figure 1, *b*. Suppression of phase separation in the InGaN layer was provided by high-temperature nitrogen-enriched growth [22]. The density of germinating dislocations in the InGaN layer was estimated from X-ray measurements at the level of $N_D \approx 6 \cdot 10^{10}\,\mathrm{cm}^{-2}$, residual electron concentration was estimated according to Hall data: $n_{\mathrm{Hall}} \approx 1.5 \cdot 10^{19}\,\mathrm{cm}^{-3}$. When registering both PL (from the front surface of the structure) and SR (from the side of the chip), the samples were pumped at a wavelength of $\lambda_{\mathrm{exc}} = 670$ nm. In the first case, a continuous-acting diode laser was used, in the second, a parametric light generator with a pulse duration of $\tau_{\mathrm{exc}} \approx 10$ ns. During SR measurements, the pump beam was focused by a cylindrical lens into a strip that completely illuminated the sample from edge to edge ($L_{\max} \approx 2.2$ mm) with a width of $\sim 120\,\mu$m. The luminescent response was analyzed by a lattice monochromator and detected by a silicon (charge-coupled device) CCD matrix. All measurements were carried out in a closed-cycle helium cryostat at a temperature of $T \approx 5$ K.

It should be noted that all measurements in this work were carried out using a time-integrating photodetector, i. e. without temporary resolution, although the considered effects of „filling“ electronic states and band gap renormal-

ization with powerful interband illumination are certainly dynamic. Here we use the fact that exciting laser pulses (≈ 10 ns) are long in comparison with the characteristic lifetimes of nonequilibrium carriers in the studied structures (< 100 ps [23]), which means that quasi-stationary pumping mode. In addition, the pumping of the active region of the structure in our experiments is significantly heterogeneous in the depth of the InGaN layer. With the absorption coefficient of exciting radiation $\alpha_{\mathrm{exc}} \approx 6 \cdot 10^4\,\mathrm{cm}^{-1}$, estimated directly from transmission measurements and in good agreement with Ref. [24], the characteristic size of the „pumped" area is $d_{\mathrm{exc}} = 1/\alpha_{\mathrm{exc}} \approx 150$ nm (see Figure 1, b). In this sense, it is possible to talk about the „renormalization of the band gap" only in terms of averaged values (however, this remark applies to the vast majority of experimental work on this issue). For III-N structures, such an approach seems justified also due to the fundamental heterogeneity of the InGaN active layer— it is well known that a highly defective elastic stress relaxation region ($\sim 100-200$ nm [25]) is always present near the InGaN/GaN interface with the buffer layer, and an accumulation layer of electrons is present at the surface ($\sim 10-20$ nm [26]). This makes it difficult for both homogeneous „pumping" of In (Ga)N layers and the correct interpretation of the data obtained. The pump wavelength chosen in this study $\lambda_{\mathrm{exc}} = 670$ nm is a compromise solution that allows, on the one hand, „to detach" from the InGaN/GaN interface, and on the other hand, to minimize the contribution of the subsurface layer to the recorded emission spectra.

3. Results and discussion

The low-temperature emission spectra of the studied sample are shown in Figure 1, a for the PL mode with weak pumping and in Figure 1, c for the SR mode with powerful pulse excitation. It can be seen that the SR line appears on the long-wavelength PL wing and shifts towards lower energies as the pumping intensity increases. The latter circumstance is generally not typical for semiconductor lasers. So, a blue shift of the generation line typically occurs in (In,Al)In GaAs structures with increasing pumping. The redshift of the SR line was repeatedly observed earlier in III nitrides, including bulk GaN [27], and was explained by the effect of band gap renormalization (although extreme pumping intensities in Ref. [27], up to $\sim 10\,\mathrm{MW/cm^2}$, may affect the interpretation of experimental data). It should also be noted that the red shift of the SR band in InGaN cannot be determined by the effects of greater reabsorption of short-wave secondary radiation as it propagates in an amplifying medium. Due to the degenerate nature of the n-InGaN ($E_{\mathrm{F}} \approx E_c + 130$ layers, meV), the SR line is significantly detached from the PL maximum and the edge of interband absorption, and the main mechanisms of optical losses determining the generation threshold are diffraction losses α_{diff} and losses on free charge carriers α_{FCA}. The total value of these losses in the studied structures is estimated at tens of cm^{-1}, and it is important here that both α_{diff} and α_{FCA} have an extremely weak spectral dependence within the SR line offset.

The evolution of the recorded SR spectra $I_{SE}(\hbar\omega)$ as the pumping intensity P_{exc} increases (Figure 1, c) can be considered within the framework of the one-dimensional optical amplifier model [28]:

$$I_{SE}(P_{\mathrm{exc}}, \hbar\omega) = \frac{A_{\mathrm{sp}}(P_{\mathrm{exc}}, \hbar\omega)}{g_{\mathrm{mod}}(P_{\mathrm{exc}}, \hbar\omega)} \times (\exp[g_{\mathrm{mod}}(P_{\mathrm{exc}}, \hbar\omega)L_{\max}] - 1). \quad (1)$$

Here A_{sp} is the spontaneous emission intensity (in arbitrary units), g_{mod} is the mode gain, $L_{\max}$ is the wavelength of radiation in the amplifying medium (actually sample size; in our case, $L_{\max} \approx 2.2$ mm). Due to the wide band of spontaneous emission, the spectral dependence A_{sp} in the expression (1) can be ignored with good accuracy (against the background of an exponential multiplier), and the intensity of spontaneous emission can be considered linear in terms of pumping power:

$$A_{\mathrm{sp}}(P_{\mathrm{exc}}, \hbar\omega) \approx \mathrm{const}(\hbar\omega) \sim (n_0 + \delta n) \times \delta p \sim P_{\mathrm{exc}}. \quad (2)$$

This implies not too intense pumping when the nonequilibrium concentrations of electrons and holes $\delta n = \delta p$ are much lower than the background concentration of electrons n_0. In addition, we do not consider excessively large pumps due to the possible influence of saturation amplification effects and consider the problem to be homogeneous along the length of the excitation region, which is one of the basic principles of applicability (1).

Within the limits of the indicated limitations, we can recalculate the measured SR spectra into gain spectra (Figure 2, a) in accordance with (1); since to correctly solve this problem, we need „calibration" absolute values of mode gain, additionally using the VSL method („variable stripe length", [28]) g_{mod} were measured at the maximum of the SR line (Figure 2, b). It should be noted that the resulting dependence $g_{\mathrm{mod}}^{\mathrm{peak}}(P_{\mathrm{exc}})$, shown in Figure 2, c, deviates from linear with sufficiently intense pumping. At the same time, even with the maximum excitation power used in this work ($P_{\mathrm{exc}}^{\max} \approx 245\ \mathrm{kW/cm^2}$), the role of saturation amplification effects remains, apparently, not very noticeable. According to Ref. [29], the criterion of „saturation" mode is the ratio $g_{\mathrm{mod}}^{\mathrm{peak}}(P_{\mathrm{exc}}^{\max}) \times L_{\max} \geq 10$; in our experiments $g_{\mathrm{mod}}^{\mathrm{peak}} \times L_{\max} < 5$. For this reason, the sublinear nature of the dependence $g_{\mathrm{mod}}^{\mathrm{peak}}(P_{\mathrm{exc}})$ can rather be explained by the intensification of nonradiative processes and warming effects. In relation to the first, the contribution of excess carriers to the rate of Auger processes the presumably dominant interband mechanism in the studied InGaN layers is further evaluated in this paper. Estimates of the heating of electrons during high-power pumping are difficult to obtain from experimental data. Since In(Ga)N emission typically occurs at the transitions „free electron–localized hole" [10], the PL and SR spectra turn out

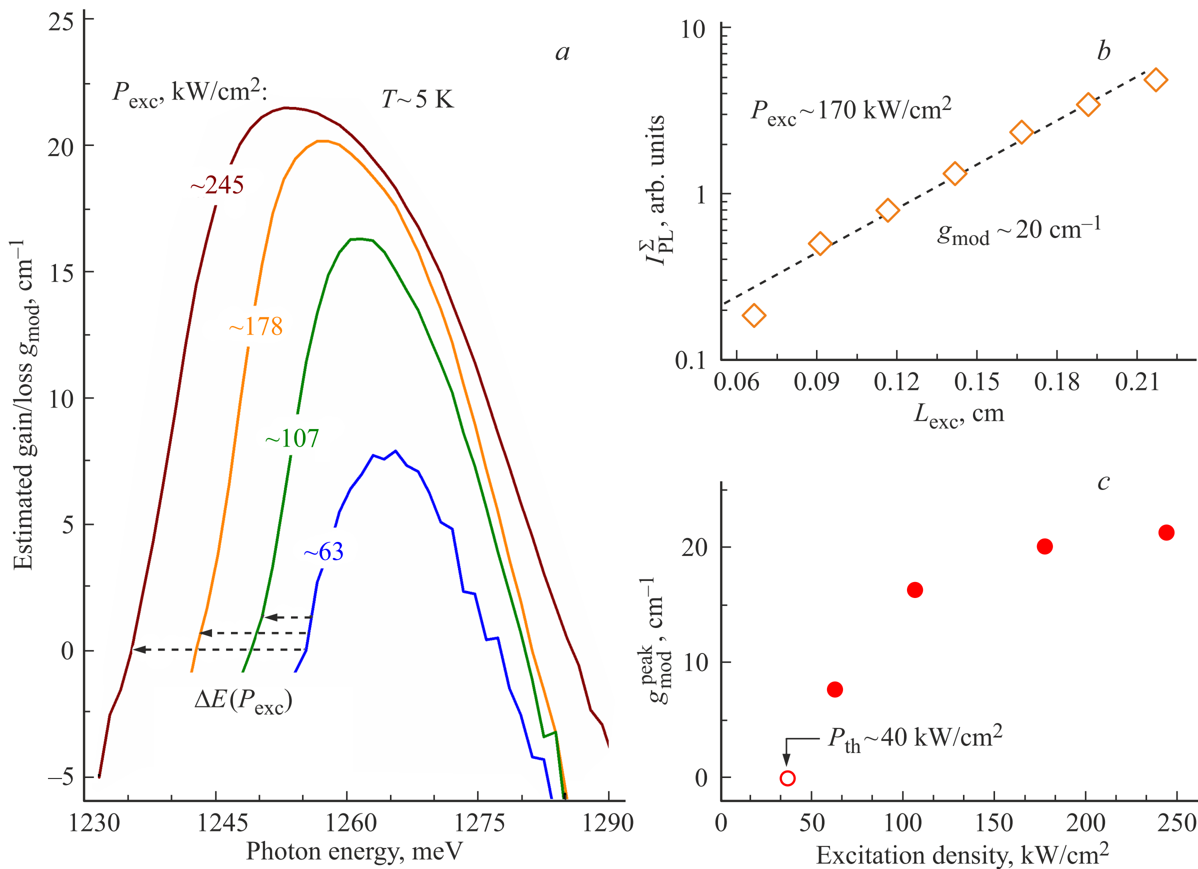

Figure 2. *a* — gain spectra at different pump intensity values, recalculated according to (1) from the measured stimulated emission spectra. *b* — estimation of the magnitude of the mode gain using the VSL method. The values of g_{mod} obtained at various P_{exc} are used for „calibration" of spectra on panel a on the ordinate scale. *c* — the magnitude of the mode gain at the maximum of the spectrum, depending on the pumping power.

to be heterogeneously broadened due to the non-thermal distribution of holes in the band potential, and, accordingly, the short-wavelength edge of the PL spectrum does not reflect the relevant electron temperature. We only note that the data on the cooling rate of hot electrons in InN [30] allow us to count on moderate heating values.

Let us now turn to the consideration of the SR spectral shift with increasing pumping power. Figure 3, *a* shows a diagram reflecting the filling of states in the conduction band with equilibrium (n_0) and excess (δn_{max}) electrons, as well as the distribution of nonequilibrium holes (p_{max}) in the valence band at maximum pumping power. The scales of the zone tails and the parameters of hole localization, as well as the value n_0 (directly in the radiating region of the structure, which differs from the „Hall" concentration averaged over the entire InGaN layer: $n_0 \approx 8 \cdot 10^{18}\,\text{cm}^{-3} < n_{Hall}$) for the studied sample were obtained by the authors earlier in Ref. [23]. At the „dark" electron concentration n_0, the Fermi level is at $\sim 130\,\text{meV}$ above the nominal bottom of the conduction band $E_c^{(0)}$, and with an increase in the nonequilibrium concentration δn it shifts upward at a rate of $dE_F/d(\delta n) \approx 1\,\text{meV}/10^{17}\,\text{cm}^{-3}$. As for nonequilibrium holes, even at maximum pumping intensity, the estimate of their concentration (for carrier lifetimes not exceeding $\tau_{PL} \approx 60\,\text{ps}$ [23]) is $p_{max} \le 1.5 \cdot 10^{18}\,\text{cm}^{-3}$. This corresponds to small (< 0.1) factors of filling localized hole states in the tail of the valence band, which means that the type of energy distribution of holes frozen in the minima of the random band potential should not noticeably depend on the pumping intensity (similar arguments for InN were given earlier, for example, in Ref. [31]). Thus, the „blue" component of the gain spectrum shift should mainly be determined by the filling of states in the conduction band (δE_F in Figure 3, *b*). At the same time, the final shift turns out to be „red" (δE_{max} in Figure 3, *b*), which indicates the predominance of the competing effect of narrowing the band gap: $|\delta E_{BGN}| > \delta E_F$.

It should be noted that due to the SR red shift with increasing excitation intensity, the pumping of the structure, which is heterogeneous in depth of the InGaN layer, does not prevent the achievement of stimulated emission. The SR line, initially detuned from interband absorption due to the Burstein-Moss shift, turns out to be even more detuned from the absorption edge in the „cold", non-pumped part of the active layer, as a result of which interband amplification in the near-surface layer of the structure competes with

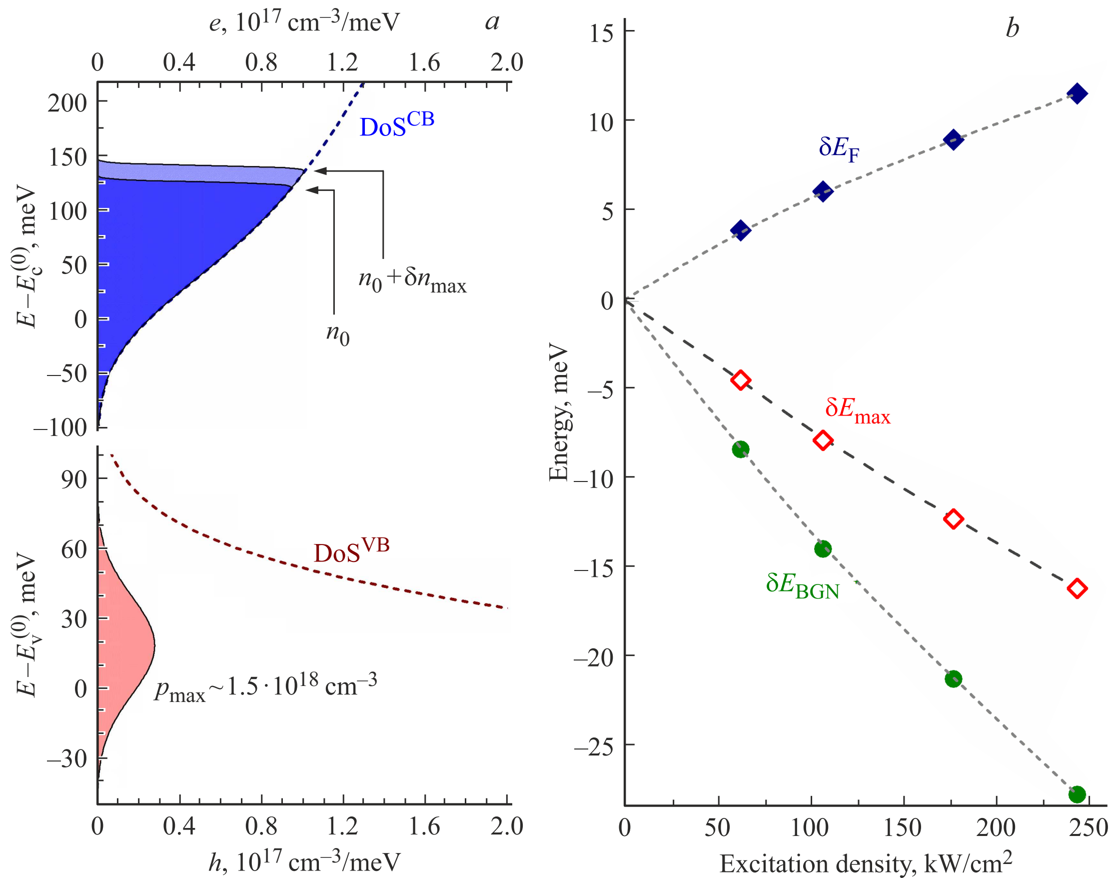

Figure 3. *a* — energy distribution of nonequilibrium electrons and holes at maximum pumping power. DoS^{CB} and DoS^{VB} is the density of states in the conduction band and valence band, taking into account the band tails; the hole distribution is considered „frozen" due to localization in band potential fluctuations. *b* — δE_{max} is the measured maximum shift in gain spectra depending on pump intensity; δE_F is the calculation of additional „filling" of conduction band due to nonequilibrium electrons; $\delta E_{BGN} \equiv \delta E_{max} - \delta E_F$ is the estimation of the magnitude of the photoinduced narrowing of the band gap.

much weaker loss mechanisms (α_{diff} and α_{FCA}), however, extending over the entire spatial scale of the waveguide mode (see Figure 1, *b*).

Next, we should recalculate the value of $\delta E_{BGN}(P_{exc})$ into the concentration dependence $\Delta E_{BGN}(\delta n)$ and compare the results with the data available in the literature. The latter for binary *n*-GaN and *n*-InN are shown in Figure 4, *a* (the energy ΔE_{BGN} is modulo magnitude postponed for convenience of comparison with the movement of the Fermi electron level ΔE_F). It should be noted that there are no well-established ideas in the literature about the contributions of specific mechanisms (exchange, correlation, and electron-impurity) interactions to the final value ΔE_{BGN}^{InN}. For this reason, we will further consider ΔE_{BGN}^{InN} as an estimate specifically for the exchange (Hartree-Fock) interaction, the most „universal" and the least sensitive to the specifics of a particular sample. It can be seen that for all background concentrations of electrons practically realized in InN ($n_0 > 2 \cdot 10^{17}\,\mathrm{cm}^{-3}$), the ratio $\Delta E_F^{InN} > \Delta E_{BGN}^{InN}$ holds, and this corresponds to the blue shift of PL and absorption spectra observed everywhere in InN as the residual electron concentration increases. For triple InGaN solutions the „compensation point" ($\Delta E_F \approx \Delta E_{BGN}$) shifts towards higher concentrations, but not too much, and in our experiments at $n_0 \approx 8 \cdot 10^{18}\,\mathrm{cm}^{-3}$ the total effect provided by with equilibrium and excess electrons, it should lead to a blue shift. At the same time, a red shift in emission is observed in the experiment, which means that the magnitude of the narrowing of the zone $\Delta E_{BGN}^{\Sigma}(\delta n)$ significantly exceeds the „exchange" correction $\Delta E_{BGN}^{*}(\delta n)$ obtained in Figure 4, *a* by linear interpolation between *n*-GaN and *n*-InN. Here, the nonequilibrium concentration of δn is estimated (Figure 4, *b*) from the balance of photogeneration and Auger recombination of excess carriers:

$$G_{exc} \equiv \frac{P_{exc}}{\hbar\omega_{pump} d_{exc}} = C_A (n_0 + \delta n)^2 \delta n \qquad (3)$$

with „calibration" of the effective Auger recombination coefficient C_A according to the PL decay time in the low-pump mode. It can be seen from Figure 4, *c* that the „hole" correction $\Delta E_{BGN}^{(e-h)} \equiv \Delta E_{BGN}^{\Sigma} - \Delta E_{BGN}^{*}$ approximately linearly depends on the nonequilibrium concentration δn in

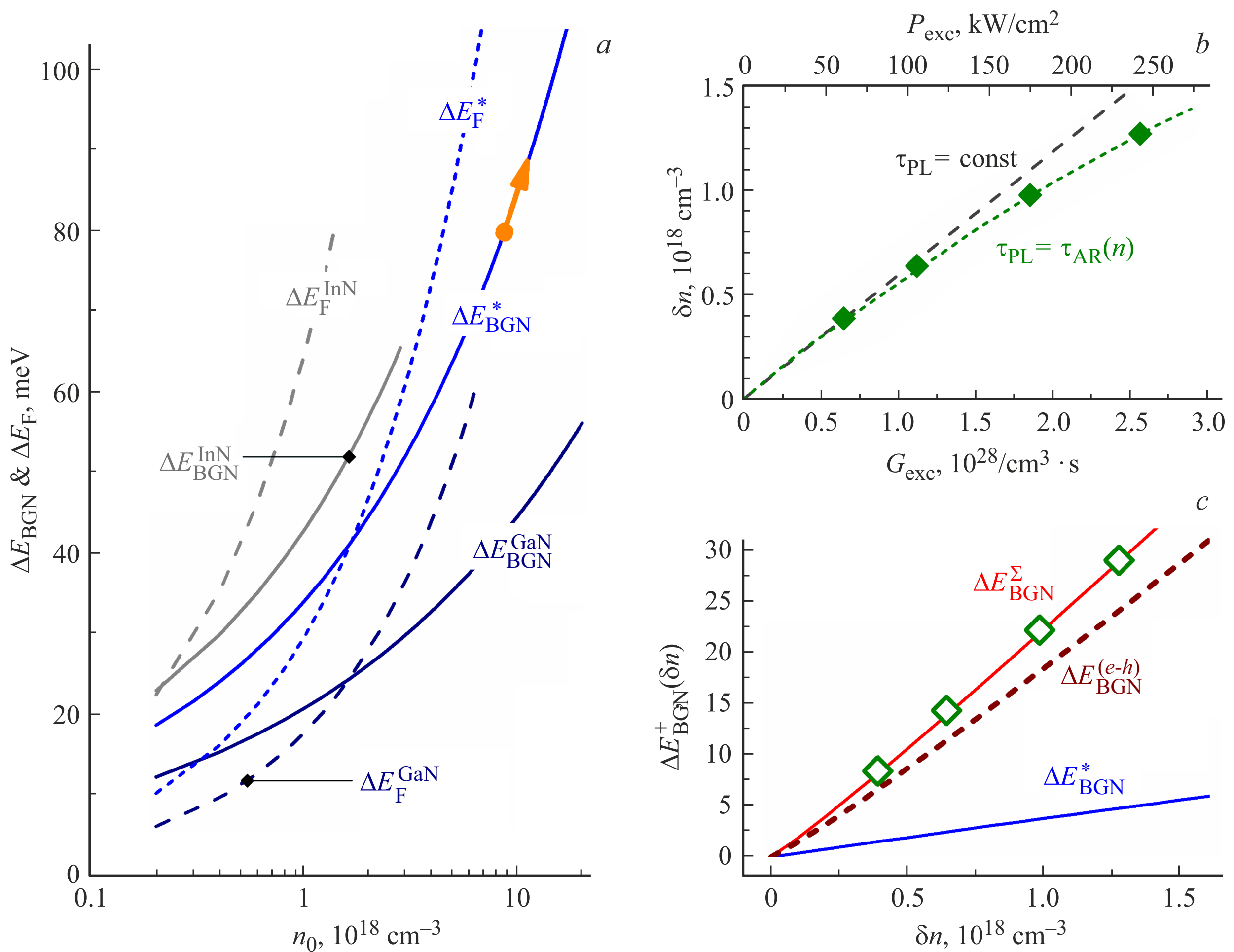

Figure 4. *a* — competition between filling of electronic states (ΔE_F) and narrowing of the band gap (ΔE_{BGN}) with a change in electron concentration in *n*-GaN and *n*-InN. The values ΔE_F^{GaN} and ΔE_F^{InN} are given by the expression $\Delta E_F = 3.58 \times (m_0/m^*)(n_0/10^{18})^{2/3}$ meV [4] for $m_{InN}^* \sim 0.05m_0$ and $m_{GaN}^* \sim 0.2m_0$, respectively. The dependency $\Delta E_{BGN}^{GaN}(n_0)$ is based on data from Ref. [7], $\Delta E_{BGN}^{InN}(n_0)$ is based on data from Ref. [11]. The dependencies ΔE_F^* and ΔE_{BGN}^* were constructed for $In_{0.6}Ga_{0.4}N$ by linear interpolation for InN and GaN. The arrow marks the „operating point" $n_0 \sim 8 \cdot 10^{18}$ cm^{-3} and its displacement in case of pumping of the sample; *b* — recalculation of the pumping power density P_{exc} into the average concentration of nonequilibrium in the excited region electrons and holes δn. Dotted line shows the estimate for a fixed carrier lifetime with low pumping ($\tau_{PL} \sim 60$ ps), symbols show the estimate taking into account the effect of nonequilibrium concentration on the rate of Auger processes. *c* — symbols: measured „dynamic" narrowing of the band gap depending on the excess concentration δn of electrons and holes, line ΔE_{BGN}^{Σ} shows the approximation of these data by the function $\propto \delta n^{\beta}$, $\beta = 1.07$. $\Delta E_{BGN}^{(e-h)}$ is the estimation of the contribution of the electron-hole interaction. The energy ΔE_{BGN}^{+} is calculated from the „dark" value $\Delta E_{BGN}^*(n_0)$.

the range under consideration $\sim (0.4-1.3) \cdot 10^{18}$ cm^{-3} and significantly exceeds the „electronic" component ΔE_{BGN}^*, reaching ~ 1.9 meV/10^{17} cm^{-3}. The following can be suggested as a possible explanation for such a noticeable effect. Nonequilibrium holes are localized in heterogeneities of the band potential at low temperatures and to some extent are analogous to charged impurities. The energy of their interaction with degenerate electrons contributes to the narrowing of the band gap, and the magnitude of this contribution can be estimated in accordance with [32]:

$$\Delta E_{e-i} = -\frac{4\pi e^2 \delta n}{\varepsilon_s a_B k_{TF}^3}. \tag{4}$$

Here ε_s is the static permittivity of InGaN, and k_{TF} is the Thomas-Fermi wave vector, which takes into account the shielding of the potential of the „impurity" by degenerate electrons. As the effective Bohr radius a_B, we can use the hole localization scale a_{loc}, estimated from the characteristic energy scale of the tail of the valence band W_h: $r_{loc}^2 = \hbar^2/2m_h W_h$. For $W_h \sim 43$ meV [23], $m_h \sim m_0$ and $\varepsilon_s \sim 6.8$ [24], the value of r_{loc} is estimated at 0.95 nm, and the resulting value $\Delta E_{e-i}/\delta n \sim 2.1$ meV/10^{17} cm^{-3} agrees well with the data in Figure 4, *c*, which indirectly indicates the acceptability of such an approach.

Within the framework of the described hypothesis, the effect of photoinduced band gap narrowing under consid-

eration can be expressed in the studied InGaN layers of „average“ compositions more strongly than in the binary InN, due to greater fluctuations in the band potential in ternary InGaN solutions [33,34] and a corresponding increase in the role of localization of nonequilibrium holes. In addition to the obvious dependence on the „operating point“ — background electron concentration n_0, which is difficult to change over a wide range, — the total value of ΔE_{BGN} should also depend on temperature, responding to the redistribution of holes in the band potential and their delocalization as we move from cryogenic temperatures to room temperature. Such a situation is difficult for a correct model description, but it may turn out to be close to the operating modes of promising InGaN structures in the red and near-infrared ranges, and temperature measurements seem to be a necessary continuation of this work aimed at detailed verification of the results obtained.

4. Conclusion

Thus, it is shown that in degenerate ($n \sim 10^{19}\,\mathrm{cm}^{-3}$) layers of ternary solutions of InGaN of „average“ compositions ($x_{\mathrm{In}} \sim 60\,\%$), the effect of narrowing the band gap during photoexcitation is strongly pronounced, the overcompensating Burstein-Moss effect, which eventually provides a red shift in the stimulated emission line as the pumping intensity increases. It is assumed that the Coulomb interaction of localized nonequilibrium holes with degenerate electrons plays a decisive role here, the contribution of which significantly exceeds the contribution of the exchange interaction of electrons to the total value ΔE_{BGN}. Taking this factor into account may be important for developing approaches to describing the characteristics of stimulated emission, analyzing gain and loss competition both in homogeneous InGaN volume layers in the mode of uneven core pumping, and in structures with a complex composition doping profile and variable band gap. The SR red shift was noted earlier for other material systems, but it is precisely for III-N structures, in which effective emission is achieved only with sufficiently strong injection due to material defects, that it may be most noticeable, including in low-dimensional InGaN structures, which are now being actively promoted towards red and IR ranges.

Funding

The study was performed using „Femtospektr“ test bench of the Center for Collective Use of the IPM RAS with the support of the Russian Science Foundation (grant No. 24-22-00320).

Conflict of interest

The authors declare that they have no conflict of interest.

References

[1] G.B. Cross, Z. Ahmad, D. Seidlitz, M. Vernon, N. Dietz, D. Deocampo, D. Gebregiorgis, S. Lei, A. Kozhanov. J. Cryst. Growth, **536**, 125574 (2020). DOI: 10.1016/j.jcrysgro.2020.125574
[2] L. Chen, S. Sheng, B. Sheng, T. Wang, L. Yang, B. Zhang, J. Yang, X. Zheng, Z. Chen, P. Wang, W. Ge, Bo Shen, X. Wang. Appl. Phys. Express, **15**, 011004 (2022). DOI: 10.35848/1882-0786/ac4449
[3] A. Imran, M. Sulaman, M. Yousaf, M.A. Anwar, M. Qasim, G. Dastgeer, K.A.A. Min-Dianey, B. Wang, X. Wang. Adv. Mater. Interf., **10**, 2200105 (2023). DOI: 10.1002/admi.202200105
[4] V. Yu, Davydov, A.A. Klochikhin, V.V. Emtsev, D.A. Kurdyukov, S.V. Ivanov, V.A. Vekshin, F. Bechstedt, J. Furthmuller, J. Aderhold, J. Graul, A.V. Mudryi, H. Harima, A. Hashimoto, A. Yamamoto, E.E. Haller. Phys. Status Solidi B, **234**, 787 (2002). DOI: 10.1002/1521-3951(200212)234:3¡787::AID-PSSB787¿3.0.CO;2-H
[5] S.C. Jain, J.M. McGregor, D.J. Roulston. J. Appl. Phys., **68**, 3747 (1990). DOI: 10.1063/1.346291
[6] S.C. Jain, D.J. Roulston. Solid-State Electron., **34**, 453 (1991). DOI: 10.1016/0038-1101(91)90149-S
[7] X. Zhang, S.-J. Chua, W. Liu, K.B. Chong. Appl. Phys. Lett., **72**, 1890 (1998). DOI: 10.1063/1.121217
[8] M. Yoshikawa, M. Kunzer, J. Wagner, H. Obloh, P. Schlotter, R. Schmidt, N. Herres, U. Kaufmann. J. Appl. Phys., **86**, 4400 (1999). DOI: 10.1063/1.371377
[9] R. Kudrawiec, M. Motyka, J. Misiewicz, B. Paszkiewicz, R. Paszkiewicz, M. Tlaczala. J. Phys. D: Appl. Phys., **41**, 165109 (2008). DOI: 10.1088/0022-3727/41/16/165109
[10] V.Yu. Davydov, A.A. Klochikhin. FTP, **38**, 897 (2004). (in Russian).
[11] S.P. Fu, T.T. Chen, Y.F. Chen. Semicond. Sci. Technol., **21**, 244 (2006). DOI: 10.1088/0268-1242/21/3/005
[12] E. Alarcon-Llado, T. Brazzini, J.W. Ager. J. Phys. D: Appl. Phys., **49**, 255102 (2016). DOI: 10.1088/0022-3727/49/25/255102
[13] F. Chen, A.N. Cartwright, H. Lu, W.J. Schaff. J. Cryst. Growth, **269**, 10 (2004). DOI: 10.1016/j.jcrysgro.2004.05.028
[14] K. Fukunaga, M. Hashimoto, H. Kunugita, J. Kamimura, A. Kikuchi, K. Kishino, K. Ema. Appl. Phys. Lett., **95**, 232114 (2009). DOI: 10.1063/1.3272916
[15] A. Mohanta, D.-J. Jang, M.-S. Wang, L.W. Tu. J. Appl. Phys., **115**, 044906 (2014). DOI: 10.1063/1.4862958
[16] Y.J. Wang, S.J. Xu, Q. Li, D.G. Zhao, H. Yang. Appl. Phys. Lett., **88**, 041903 (2006). DOI: 10.1063/1.2168035
[17] G. Xu, G. Sun, Y.J. Ding, H.-P. Zhao, G. Liu, J. Zhang, N. Tansu. J. Appl. Phys., **113**, 033104 (2013). DOI: 10.1063/1.4775605
[18] D. Iida, K. Ohkawa. Semicond. Sci. Technol., **37**, 013001 (2022). DOI: 10.1088/1361-6641/ac3962
[19] P. Li, H. Li, M.S. Wong, P. Chan, Y. Yang, H. Zhang, M. Iza, J.S. Speck, S. Nakamura, S.P. Denbaars. Crystals, **12**, 541 (2022). DOI: 10.3390/cryst12040541
[20] X. Zhao, Ke Sun, S. Cui, B. Tang, H. Hu, S. Zhou. Adv. Photon. Res., **4**, 2300061 (2023). DOI: 10.1002/adpr.202300061
[21] T.H. Ngo, B. Gil, B. Damilano, K. Lekhal, P. de Mierry. Superlatt. Microstruct., **103**, 245 (2017). DOI: 10.1016/j.spmi.2017.01.026

[22] D.N. Lobanov, M.A. Kalinnikov, K.E. Kudryavtsev, B.A. Andreev, P.A. Yunin, A.V. Novikov, E.V. Skorokhodov, Z.F. Krasilnik. FTP, **58**, 220 (2024). (in Russian). DOI: 10.61011/FTP.2024.04.58547.6357H
[23] K.E. Kudryavtsev, D.N. Lobanov, M.A. Kalinnikov, A.V. Novikov, B.A. Andreev, Z.F. Krasilnik. Pisma ZhETF, **121**, 688 (2025). (in Russian). DOI: 10.31857/S0370274X25040234
[24] S.A. Kazazis, E. Papadomanolaki, M. Androulidaki, M. Kayambaki, E. Iliopoulos. J. Appl. Phys., **123**, 125101 (2018). DOI: 10.1063/1.5020988
[25] V. Lebedev, V. Cimalla, J. Pezoldt, M. Himmerlich, S. Krischok, J.A. Schaefer, O. Ambacher, F.M. Morales, J.G. Lozano, D. Gonzalez. J. Appl. Phys., **100**, 094902 (2006). DOI: 10.1063/1.2363233
[26] T.D. Veal, I. Mahboob, L.F.J. Piper, C.F. McConville, H. Lu, W.J. Schaff. J. Vac. Sci. Technol. B, **22**, 2175 (2004). DOI: 10.1116/1.1771672
[27] S. Hess, R.A. Taylor, J.F. Ryan, B. Beaumont, P. Gibart. Appl. Phys. Lett., **73**, 199 (1998). DOI: 10.1063/1.121754
[28] K.L. Shaklee, R.F. Leheny. Appl. Phys. Lett., **18**, 475 (1971). DOI: 10.1016/0022-2313(73)90072-0
[29] L. Dal Negro, P. Bettotti, M. Cazzanelli, D. Pacifici, L. Pavesi. Optics Commun., **229**, 337 (2004). DOI: 10.1016/j.optcom.2003.10.051
[30] S.-Ze Sun, Yu-C. Wen, S.-H. Guol, H.-M. Lee, S. Gwo, C.-K. Sun. J. Appl. Phys., **103**, 123513 (2008). DOI: 10.1063/1.2940737
[31] S.P. Fu, Y.F. Chen, K. Tan. Solid State Commun., **137**, 203 (2006). DOI: 10.1016/j.ssc.2005.11.013
[32] J. Wu, W. Walukiewicz, W. Shan, K.M. Yu, J.W. Ager III, E.E. Haller, Hai Lu, W.J. Schaff. Phys. Rev. B, **66**, 201403 (2002). DOI: 10.1103/PhysRevB.66.201403
[33] D.S. Arteev, A.V. Sakharov, E.E. Zavarin, W.V. Lundin, A.N. Smirnov, V.Yu. Davydov, M.A. Yagovkina, S.O. Usov, A.F. Tsatsulnikov. J. Phys.: Conf. Ser., **1135**, 012050 (2018). DOI: 10.1088/1742-6596/1135/1/012050
[34] S.A. Kazazis, E. Papadomanolaki, E. Iliopoulos. J. Appl. Phys., **127**, 225701 (2020). DOI: 10.1063/1.5128448

Translated by A.Akhtyamov